| JMATPRO | Journal of Advanced Materials and Processing<br>11 (2): 55-64, Spring 2023<br>http://sanad.iau.ir/journal/jmatpro<br>Doi: 10.71670/jmatpro.2024.1122429 |
|---|---|

Research Paper

# Effect of Filler Metal Type on the Microstructure of Welded Joints of HP Heat-Resistant Steel Modified by Niobium

**Jamal Hussain Mansoor, Reza Dehmolaei*, Mostafa Eskandari, Seyed Reza Alavi Zaree**
*Department of Materials Science & Engineering, Faculty of Engineering, Shahid Chamran University of Ahvaz, Ahvaz, Iran.*

**ARTICLE INFO**

*Article history:*

Received 11 June 2024
Accepted 20 August 2024
Available online 1 May 2023

*Keywords:*
*filler metal*
*microstructure*
*interface*
*weld metal*
*unmixed zone*
*epitaxial growth*

**ABSTRACT**

In this research, HP heat-resistant steel modified by niobium was welded using the GTAW process and ER NiCr-3, ER NiCrMo-3, and MF filler rods. The microstructure of the base metal, weld metals, heat-affected zone, and interface between the base and weld metals was studied using optical and electron microscopes (FESEM) equipped with an EDS point analysis system. The microstructure of HP steel base metal with an austenitic matrix and chromium-rich and niobium-rich precipitates on the grain boundary was observed. All three weld metal microstructures have a fully austenitic matrix that is dendritically solidified. In all weld metal produced by three different weld wires, precipitates rich in chromium ($M_{23}C_6$ carbide) and precipitates rich in niobium and titanium (MC carbide) were observed. The microstructural studies showed that the interfaces between the base metal and weld metals are fully continuous and free of cracks and voids. An unmixed zone (non-homogeneous zone) with a large width was formed at the interface between the base metal and the ERNiCr-3 weld metal. Any unmixed zone was not observed at the interface of the base metal and weld metals of the ERNiCrMo-3 and MF steel. Epitaxial growth was observed at the interface between the base metal and weld metals of ER NiCrMo-3 and MF steel.

**Citation**: Hussein Mansoor, J.; Dehmolaei, R.; Eskandari, M.; Alavi Zaree, S.R. (2023). Effect of Filler Metal Type on the Microstructure of Welded Joints of HP Heat-Resistant Steel Modified by Niobium, Journal of Advanced Materials and Processing, 11 (2), 55-64. Doi: 10.71670/jmatpro.2024.1122429



* **Corresponding Author:**
E-Mail: Dehmolaei@scu.ac.ir

## 1. Introduction

The HP heat-resistant steel, due to its excellent creep resistance, high-temperature endurance, and thermal fatigue resistance, is widely used in the construction of high-temperature equipment such as natural gas cracking tubes, ethylene cracking furnace tubes, pyrolysis furnace tubes, and heat treatment baskets [1–3]. The incorporation of elements like niobium and titanium into the chemical composition of these steels, which produces more stable carbides of TiC and NbC instead of chromium carbides, has enhanced their creep resistance [4, 5]. Welding processes such as GTAW and SMAW are used for joining this alloy, as well as for dissimilar welding to other alloys [2, 6]. In casting conditions, HP heat-resistant steel has excellent ductility and weldability. Nevertheless, controlling the microstructure and grain size of the weld metal has an important role in the mechanical properties (strength, ductility, and toughness) and susceptibility to hot cracking of weld joints [7]. Besides welding process parameters such as heat input and chemical composition of base and filler metals, the application of external vibration (electromagnetic, ultrasonic, and mechanical) has an important role in controlling the weld metal microstructure and grain size and decreasing the sensitivity to hot cracking [7–8]. Among these parameters, the correct choice of filler metal plays an important role in reducing sensitivity to hot cracking, removing discontinuities such as the unmixed zone near the fusion line, and reducing grain boundary migration in the weld metal [9–10]. When choosing the filler metal, parameters such as the chemical composition difference, the melting point, the coefficient of thermal expansion, and its metallurgical compatibility with the base metal, as well as economic aspects, must be considered [9, 11]. Nickel-based superalloys such as Inconel 82 are used as filler metal in HP heat-resistant steel weld joints due to their excellent creep and oxidation resistance and suitable thermal expansion coefficient [11, 6]. The use of such filler metals is often associated with problems such as grain boundary migration in the weld metal and the formation of an unmixed zone in the HAZ near the fusion line [9–12]. One of the major issues with using Inconel 82 filler metal in the production of HP heat-resistant steel weld joints is the formation of the unmixed zone [8–9]. The unmixed zone is a boundary layer near the fusion line, which is formed by the melting of the base metal and its solidification without mechanical mixing with the weld metal [14, 13, 9]. The unmixed zone is often formed in weld joints where the melting range of the filler metal is close to or higher than that of the base metal [14]. In environments where the base and weld metals have good corrosion resistance, the unmixed zone is a preferred place for corrosion [13, 15, 16]. In our research, the effect of the type of filler metal on the microstructure of HP heat-resistant steel weld joints produced using the GTAW process has been studied and investigated.

## 2. Material and Methods

In this research, cast HP heat-resistant steel, separated from the reformer tubes of direct reduction units of iron production, was used as the base metal. Samples were cut from HP steel reformer tubes with a thickness of 18 mm. All pieces were machined from a thickness of 18 mm to a thickness of 12 mm. Inconel 82 (ERNiCr-3), Inconel 625 (ERNiCrMo-3), and weld wire similar to the base metal (MF) were used as filler metals. The chemical composition of base and filler metals is shown in Table 1. For welding, samples with dimensions of 100 x 100 x 12 $mm^3$ were separated from the base metal. The joint design was prepared in the form of a V groove with an angle of 75º and a root opening of 2 mm. The welding was carried out by the gas tungsten arc welding process (GTAW) during six passes with different filler metals. During welding, argon gas with a purity of 99.99% was used as a protection gas. Welding parameters, including a current of 125A intensity, a voltage of 14V, an average welding speed of 1.13 mm/s, and an average heat input of 0.97 kJ/mm, were used for different welds. To study the microstructure, different samples were taken from the base metal, weld metal, and interface of weldments. The samples were polished after sanding with 60 to 3000 grits using 0.03 and 0.05-micron alumina powder. Then, the samples were electro-etched with 10% oxalic acid (10 grams of oxalic acid and 100 ml of distilled water) under a voltage of 26 volts for 25 seconds. Different weld zones consisting of base, weld metal, and heat-affected zone were studied and analyzed using an optical microscope and a field emission scanning electron microscope (FESEM) equipped with a point analysis system (EDS).

## 3. Results and Discussion

### 3.1. Microstructure

#### 3.1.1. Base metal microstructure

Figure (1) shows the optical and FESEM images of the microstructure of the cast HP heat-resistant steel. From Figure 1-a, it can be seen that the microstructure of this steel includes an austenitic matrix along with a continuous network of primary eutectic carbides on the grain boundaries. The FESEM image (Figure 1-b) clearly shows the presence of two different types of precipitates with dark and bright colors. The difference in the color of the precipitates can be due to the difference in the atomic weight of the elements that exist in them. The results of EDS analysis (Figures 1-c and 1-d) show that the dark precipitates are rich in carbon and chromium along with some amounts of iron, which

can be $M_{23}C_6$ carbide (M indicates chromium along with small amounts of iron), and bright precipitates are rich in carbon and niobium carbide, which can be NbC (the other elements such as iron, chromium, and nickel have been gotten from the matrix.

### 3.2.1. Weld metal microstructure

The microstructure of weld metals is shown in Figures 2–5. Figure (2) shows optical and FESEM images of the precipitates from the ERNiCr-3 weld metal, along with the EDS analysis. The figure shows that the ERNiCr-3 weld metal has a dendritic microstructure with a fully austenitic matrix. The austenitic matrix of this weld metal is due to no allotropic transformation of the weld metal after solidification and during cooling to ambient temperature. Figure 2-a shows that intense grain boundary migration has occurred in the weld metal's microstructure. Migrated grain boundaries (MGB) are obtained from solidification grain boundaries (SGB) with a high deviation in orientation. The driving force of grain boundary migration is the growth of simple grains in base metals. Grain boundary migration is one of the defects in this weld metal, and some segregation along them can occur with the sweeping mechanism [17]. In the electron microscope image (Figure 2-b), two types of precipitates with dark and white colors can be seen in the weld metal. The EDS analysis of these precipitates in Figure 2-c shows that the dark precipitates are mostly rich in chromium, along with amounts of carbon that can be chromium-rich carbides ($M_{23}C_6$). These precipitates are formed due to the presence of carbon and high amounts of chromium in the filler metal (Table 1) after solidification and during cooling of the weld metal in the temperature range of chromium carbide stability (650–900 °C) [17]. Figure 2-d shows that the bright phases with nearly spherical morphology are rich in niobium, which could be niobium carbide (NbC). Niobium, which exists in wire filler metal, has a strong chemical affinity with carbon, resulting in the formation of NbC during the solidification and cooling of the weld metal [9, 18].

**Table 1.** Chemical composition of base and filler metals (wt%)

| Fe | Ni | Cr | C | Nb | Ti | Al | Mo | Mn | Si | |
|---|---|---|---|---|---|---|---|---|---|---|
| 35.4 | 35.8 | 24.4 | 0.4 | 1.3 | ---- | ---- | 0.04 | 1.3 | 1.3 | HP Steel |
| 3 | 67 | 18.2 | 0.1 | 2-3 | 0.75 | 0.3 | ---- | 2.5 | 0.5 | ERNiCr-3 |
| 5 | 58 | 22 | 0.1 | 3.15 | 0.4 | 0.4 | 10 | 0.5 | 0.5 | ERNiCrMo-3 |
| 35.1 | 35.0 | 24.3 | 0.46 | 1.3 | ------ | ----- | 0.3 | 1.25 | 1.55 | AM (Matching Filler) |

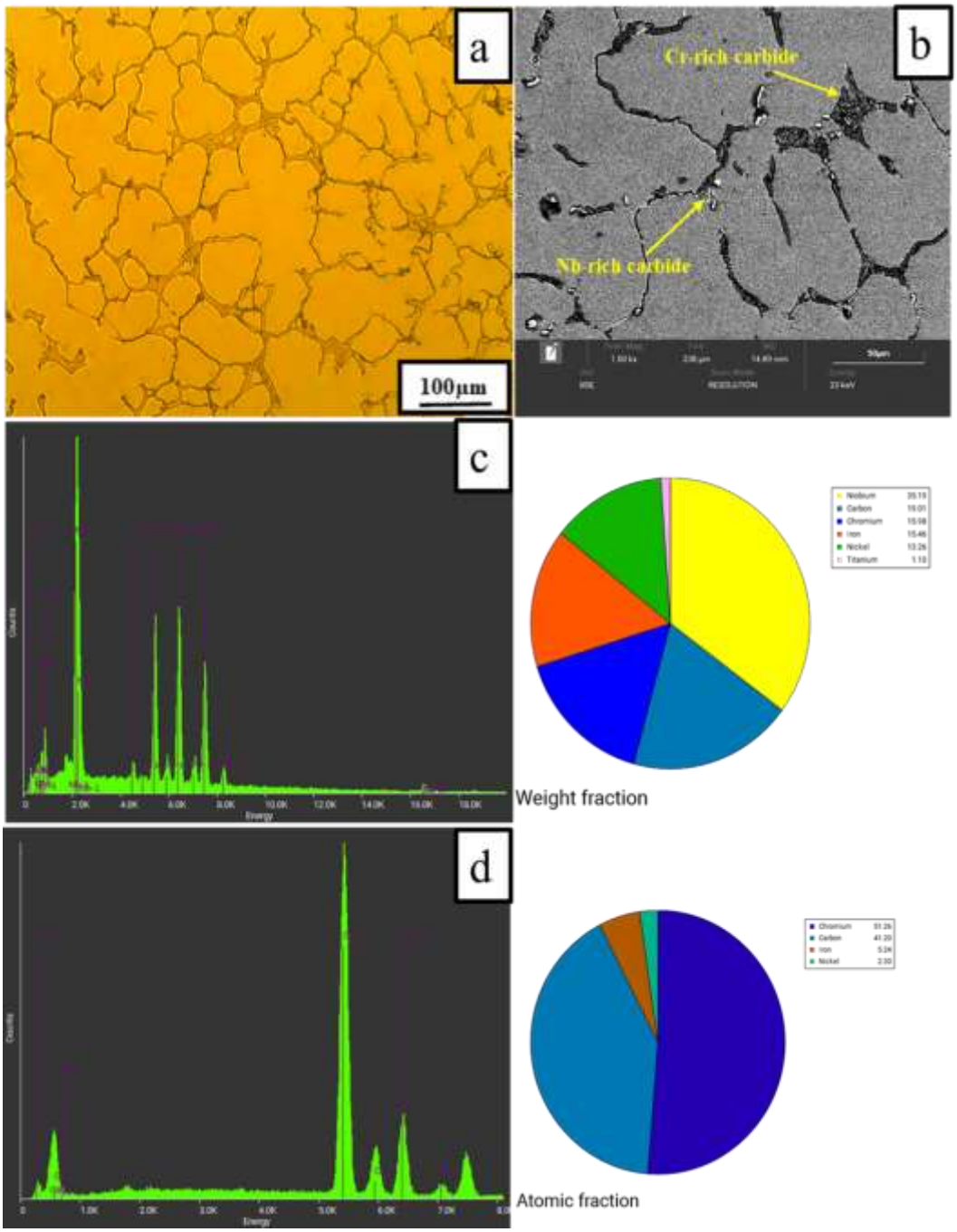


**Fig. 1.** Optical and FESEM images and the EDS analysis of precipitates of the microstructure of HP heat-resistant steel. a) Optical image, b) FESEM image, c) EDS analysis of white precipitates (NbC), d) EDS analysis of dark precipitates ($Cr_{23}C_6$)

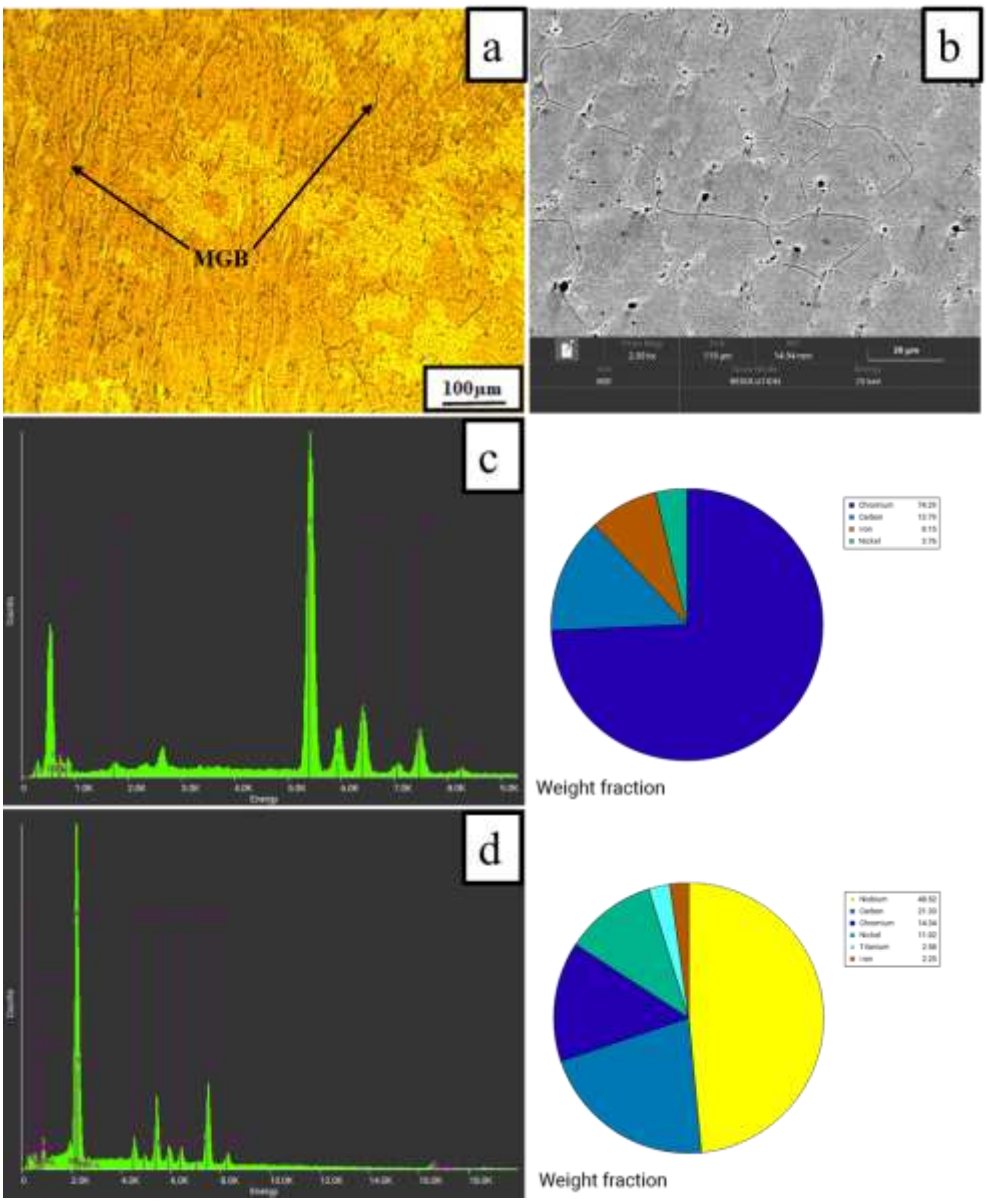


**Fig. 2.** Weld metal images of ERNiCr-3 a) Optical image, b) FESEM image, c) EDS analysis of dark precipitates ($Cr_{23}C_6$), and d) EDS analysis of white precipitates (NbC)

Figure 3 shows the optical and FESEM images of the microstructure of ERNiCrMo-3 weld metal. It can be seen that the structure of the weld metal is completely austenitic, which was dendritically solidified. The images show that different precipitates have formed along the boundaries and within the grains. Comparing Figure 3-a with Figure 2-a reveals a significant reduction in grain boundary migration in the microstructure of ERNiCrMo-3 weld metal, when compared to ERNiCr-3 weld metal. Indeed, the presence of precipitates on the solidification grain boundaries (SGB) and solidification subgrain boundaries (SSGB) causes the crystallographic component of the solidified boundaries to be locked and therefore prevents the migration of the boundaries in this weld metal [18].

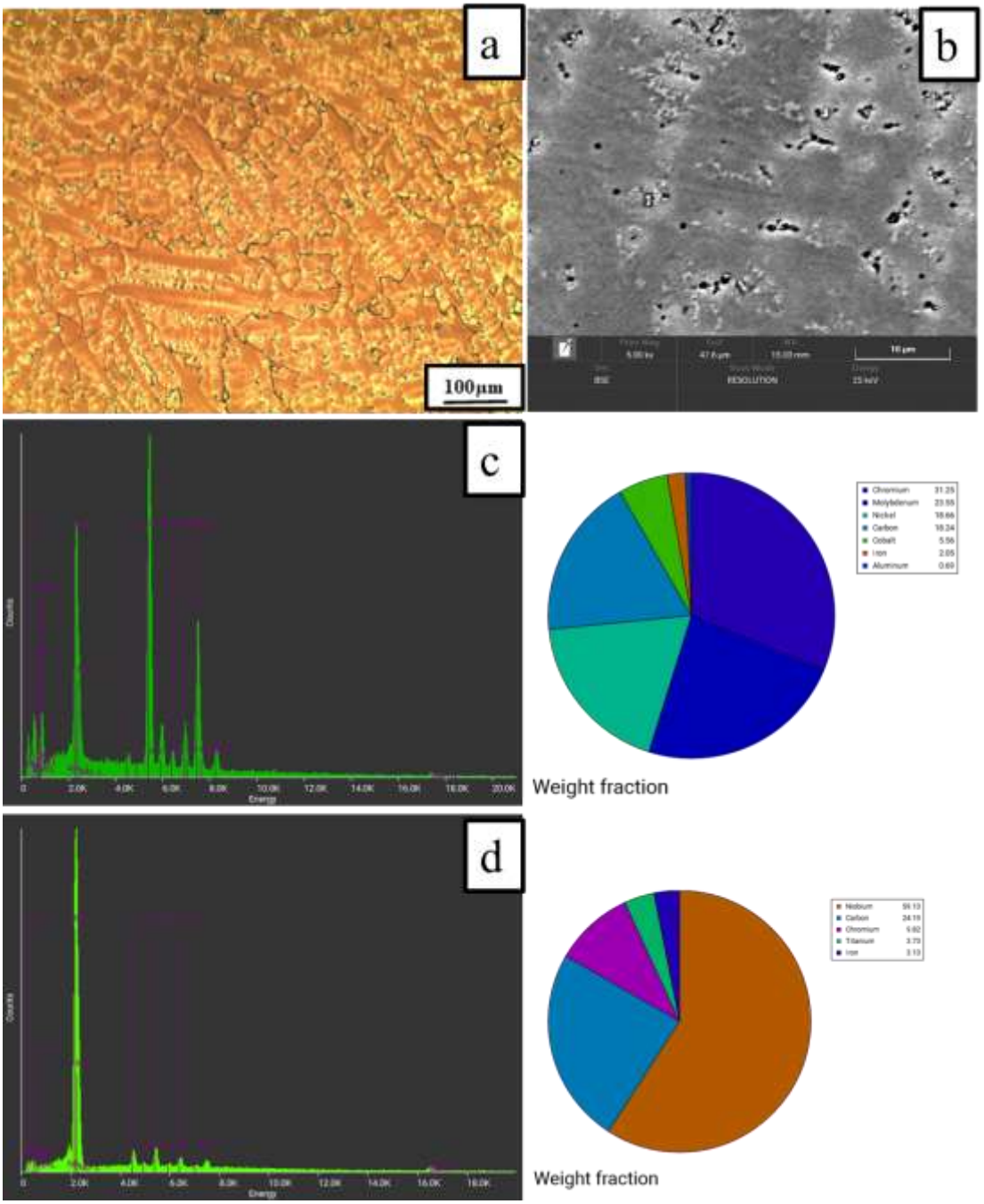


**Fig. 3.** Weld metal images of ERNiCrMo-3 a) optical image, b) FESEM image, c) EDS analysis of dark precipitates d) EDS analysis of white precipitates

In Figure 3-b (FESEM image), dark and white precipitates are obviously seen. The EDS analysis of the precipitates in Figures 3-c and 3-d shows that the white precipitates are rich in niobium, titanium, and carbon, which can be MC carbides (M: niobium and some amounts of titanium), and the dark precipitates are rich in chromium, carbon, and molybdenum, which can be $M_{23}C_6$ carbides (M: chromium along with molybdenum amounts). The presence of niobium, titanium, chromium, and molybdenum elements in the composition of the weld metal is the main factor of precipitates formation within the weld metal during the solidification and cooling to the ambient temperature.

The microstructure of MF weld metal and the analysis of its precipitates are shown in Figure 4. Figure 4-a shows that the microstructure of HP weld metal is completely austenitic and dendritically solidified. In the figure, solidification boundaries and subgrain boundaries are clearly visible. A comparison of Figure 4-a and Figure 2-a reveals that no obvious grain boundary migration occurred in MF weld metal. Studying the weld metal with an electron microscope (FESEM) in Figure 4-b shows that many precipitates in the weld metal with dark colors (mainly on the grain boundary) and white (on the grain boundary and within the grains) have been formed. The results of the EDS analysis of the

precipitates in Figures 4-c and 4-d show that the dark precipitates are rich in chromium and carbon, which can be chromium carbide $M_{23}C_6$, where M is chromium, along with amounts of iron, and the white precipitates are rich in carbon and niobium, which can be in the form of niobium carbide NbC (niobium carbides are very fine; for this reason, the other elements, such as iron, chromium, and nickel, have been gotten from the matrix).

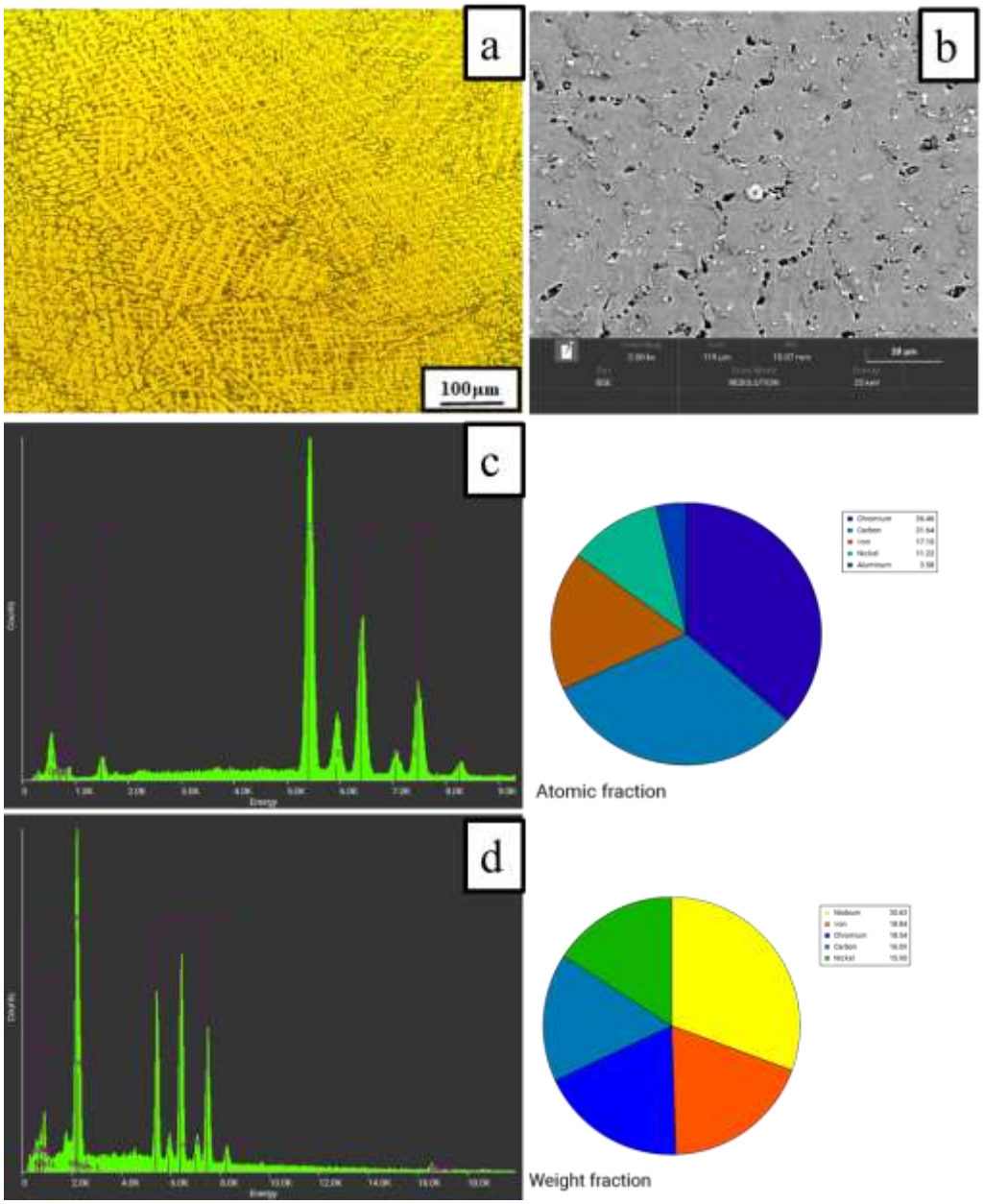


**Fig. 4.** Weld metal images of MF filler wire a) optical image, b) FESEM image, c) EDS analysis of dark precipitates, and d) EDS analysis of white precipitates

### 3.1.3. The HAZ microstructure and the interface of the base and weld metals

Figure 5 shows the optical and FESEM images of the base metal interface with the ERNiCr-3 weld metal. Figures 5-a and 5-b show that the joint interface is completely continuous and no cracks or voids are observed. On the joint interface and near the fusion line, a heterogeneous area with a large width and dendritic structure is observed. Further study by electron microscopy (FESEM) in Figure 5-b has also confirmed the presence of this inhomogeneous area with a large width. The results of linear EDS analysis of the joint interface (Figure 5-c) show that this area has a chemical composition similar to the base metal. Therefore, this zone can be considered an unmixed zone. The unmixed zone is usually formed when the melting point of the filler metal is close to or higher than the melting point of the base metal [13–19]. The melting temperature range of HP steel base metal (1340–1355 °C) and the melting temperature range

of ERNiCr-3 filler metal (1340–1348 °C) are very close to each other, so an unmixed zone for them can be formed easily [20]. On the interface of the joint near the base metal, the grains detached from the base metal are also clearly observed. These grains are also detached from the base metal as a result of grain boundaries melting (areas with a melting point lower than the grains). They are not melted due to insufficient temperature, and without entering the weld pool, a primary and distinct form near the grains of the base metal is observed.

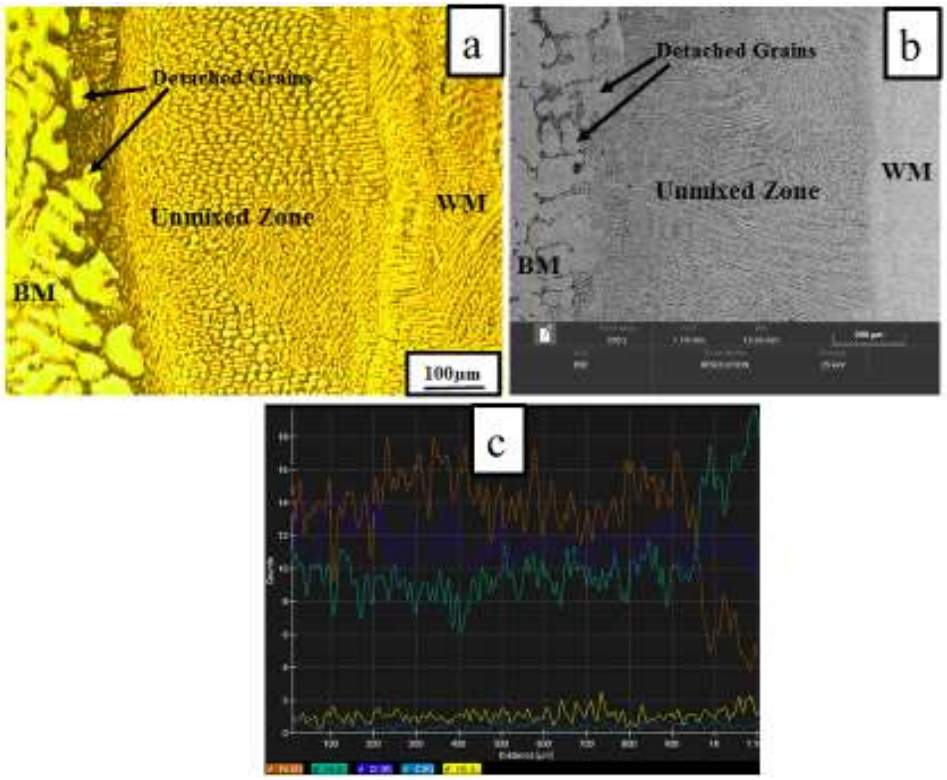


**Fig. 5.** Interface images of the base metal and ERNiCr-3 weld metal, a) Optical image b) FESEM image, and c) EDS linear analysis results

Figure 6 shows the interface between the base metal and the ERNiCrMo-3 and MF weld metals. Figures 6-a and 6-b show that the interface between the base metal and the ERNiCrMo-3 weld metal is completely continuous, and no cracks, voids, or discontinuities are observed. The figure shows that the unmixed zone is not formed in the interface produced by ERNiCrMo-3 filler metal, and complete mixing between the weld pool and the melted base metal has taken place. It can be seen from the figure that grain growth occurred in HAZ near the fusion line. It can also be observed that epitaxial growth occurs when the base metal grains in the vicinity of the fusion line start growing toward weld metal. As a result of this epitaxial growth, type I boundaries are observed, which continue in the direction perpendicular to the fusion line from the interface to the inside of the weld metal. Images 6-c and 6-d show that the interface between the base metal and the MF weld metal is also completely continuous and free of any cracks and discontinuities. At this interface, the epitaxial growth can be seen more clearly. The similarity of the chemical composition of the base and filler metals is the main factor in the epitaxial growth at this interface. In this joint, due to the high heat input of the welding process, grain growth has also occurred. Comparing Figures 5-a and 6-c, it can be seen that no unmixed zone on the joint interface was formed for MF filler metal.

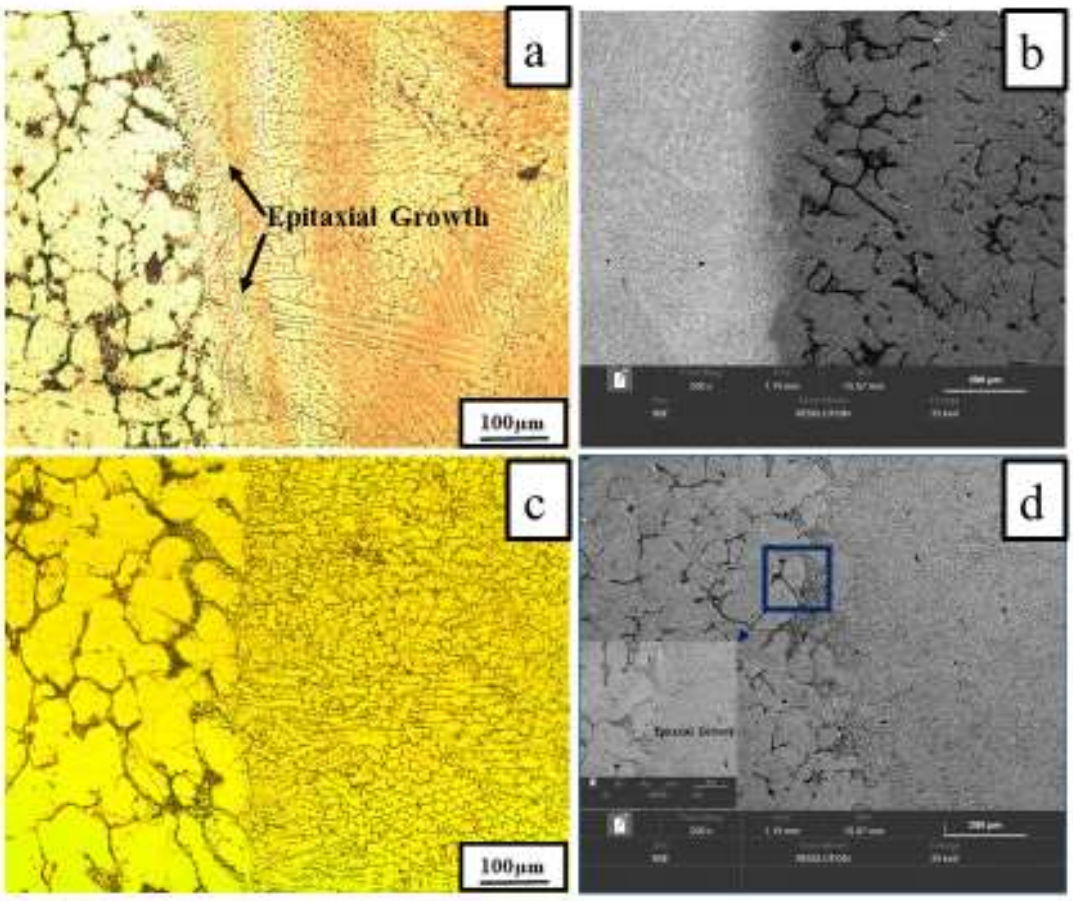


**Fig. 6.** Optical and FESEM images of interface between the base metal and weld metals a) ERNiCrMo-3, and b) MA filler metal

## 4. Conclusion

The results of this research are presented below.

1. The microstructure of all three weld metals, ERNiCr-3, ERNiCrMo-3, and MF, was observed to be fully dendritic with an austenitic matrix along with $M_{23}C_6$ and MC carbide precipitates.
2. The interface between the base metal and all three weld metals was observed to be completely continuous and free of any cracks or voids.
3. At the interface between the base metal and ERNiCr-3 weld metal, an unmixed zone with a large width was observed. At this interface, semi-melted grains detached from the base metal were observed.
4. For ERNiCrMo-3 and MF filler metals, the unmixed zone was not observed at the interface. At these interfaces, epitaxial growth and type I boundaries were observed. In addition, at these interfaces near the fusion line, grain growth was observed.

## References

[1] Siqueira de NC, Arenas MP, de Almeida PD, Araújo LS, Eckstein CB, Nogueira Jr L, de Almeida LH, Pereira GR. Characterization of the aging state of modified HP steels by ultrasonic signal processing and the effect of creep voids in the interdendritic region. Journal of Materials Research and Technology. 2018;7(3):361-5.

[2] Shinozaki K, Kuroki H, Nakao Y, Nishimoto K, Inui M, Takahashi M. Deterioration of weldability of long-term aged HP heat-resistant cast steel containing Nb, Mo, and W. Welding international. 1999;13(1):39-48.

[3] Rampat K, Maharaj C. Creep embrittlement in aged HP-Mod alloy reformer tubes. Engineering Failure Analysis. 2019; 100:147-65.

[4] Almeida de Soares GD, de Almeida LH, da Silveira TL, Le May I. Niobium additions in HP heat-resistant cast stainless steels. Materials Characterization. 1992;29(3):387-96.

[ 5] Barbabela GD, de Almeida LH, da Silveira TL, Le May I. Role of Nb in modifying the microstructure of heat-resistant cast HP steel. Materials characterization. 1991;26(3):193-7.

[6] Hsieh CC, Lai CH, Wu W. Effect of vibration on microstructures and mechanical properties of 304 stainless steel GTA welds. Metals and materials international. 2013; 19:835-44.

[7] Kou SD. Welding Metallurgy, New Jersy. USA. 2003;431(446):223-5.

[8] Dehmolaei R, Shamanian M, Kermanpur A. Effect of electromagnetic vibration on the unmixed zone formation in 25Cr–35Ni heat resistant steel/Alloy 800 dissimilar welds. Materials characterization. 2008; 59(12):1814-7.
[9] Dehmolaei R, Shamanian M, Kermanpur A. Microstructural characterization of dissimilar welds between alloy 800 and HP heat-resistant steel. Materials Characterization. 2008;59(10):1447-54.
[10] Dehmolaei R, Shamanian M, Kermanpur A. Factors affecting weldability improvement of dissimilar welds of aged HP stainless steel and alloy 800. International Journal of Iron & Steel Society of Iran. 2008;5(1):15-21.
[11] Sireesha M, Shankar V, Albert SK, Sundaresan S. Microstructural features of dissimilar welds between 316LN austenitic stainless steel and alloy 800. Materials Science and Engineering: A. 2000;292(1):74-82.
[12] Cui Y, Xu CL, Han Q. Effect of ultrasonic vibration on unmixed zone formation. Scripta materialia. 2006; 55(11):975-8.
[13] Lu Q, Chen L, Ni C. Improving welded valve quality by vibratory weld conditioning. Materials Science and Engineering: A. 2007;457(1-2):246-53.
[14] Baeslack WA, Lippold JC, Savage WF. Unmixed zone formation in austenitic stainless steel weldments. Welding Journal. 1979 Jun;58(6):168.
[15] Garner A. Corrosion of high alloy austenitic stainless steel weldments in oxidizing environments. Mater Perform 1982;21:9–14.
[16] Tuthill AH. Problems involved in testing for corrosion susceptibility in stainless steel welds are reviewed, and guidance is offered. Weld J. 2005;84(5):36-40.
[17] Lippold JC, Kotecki DJ. Welding metallurgy and weldability of stainless steels Lippold JC, Kotecki DJ. Welding metallurgy and weldability of stainless steels, John Wiley & Sons, Inc, 2005.
[18] Lippold JC. Welding metallurgy and weldability. John Wiley & Sons; 2014 Nov 24.
[19] Lukkari J, Moisio T. The Effect of the Welding Method on the Unmixed Zone of the Weld. Microstructural Science. 1979; 7:333-44.
[20] Metals Handbook, Properties and Selection: Stainless Steels, Tool Materials and Special-Purpose Metals, Vol. 3, 9th Edition; 1980.